Mediterranean Archaeology and Archaeometry, Vol. 5, No 2, pp. 75-91

REVIEW AND SOFTWARE ASSESSMENT OF THE RECENT SIMS-SS OBSIDIAN HYDRATION DATING METHOD

IOANNIS LIRITZIS*

Laboratory of Archaeometry
Dept. of Mediterranean Studies
University of the Aegean, 1 Demokratias Ave.
Rhodes 85100, Greece (liritzis@rhodes.aegean.gr)

THEODORE GANETSOS
NIKOLAOS LASKARIS

Dept. of Electronics
Technical Educational Institute (TEI) of Lamia
Lamia, Greece

** to whom all correspondence should be addressed*

Received: 30 – 6- 2005
Accepted: 26 – 11 - 2005

ABSTRACT

The hydration dating of obsidian tools employing the recent method of SIMS-SS has been further re-evaluated with regards to a novel in-house software (using MATLAB) and refinement of the procedure for the location of the surface saturation layer (SS). The latter is defined from a combination of linear regressions (for the determination of the constant concentration level) and two derivatives of the polynomial fitting of the whole and initial sigmoid profile of Concentration versus Hydration depth (x), derived by SIMS. The derivation of age equation is reviewed following a detailed presentation of formulas and prevailed conditions. Four dates are produced with the new software from the Aegean, Mexico and Easter Islands, compared to earlier calculations. In all cases the calculated ages is concordant with the expected archaeological ages.

KEYWORDS: SIMS, obsidian, dating, surface saturation, diffusion, Fick's law, SIMS-SS, software

INTRODUCTION

The obsidian hydration dating (OHD) method is based upon modeling the rate of water diffusion into a natural glass surface and establishing a diffusion coefficient for this process. It is accepted that the rate of water diffusion, the diffusion coefficient, is exponentially dependent on temperature and exhibits an Arrhenius type behavior. A variety of strategies have been developed over the years to calibrate the movement of ambient water into a glass. Many of these approaches have developed procedures for controlling the chemical composition of the glass and modeling the environmental history of the artifact context (e.g., temperature, humidity) (Friedman & Long 1976; Mazer et al., 1991; Stevenson et al., 2002).

However, the development of calibrations to compensate for variation in external variables has proven to be difficult. This has been the major impediment to making OHD a fully chronometric dating method comparable to radiocarbon dating.

The new dating method developed by Liritzis and Diakostamatiou (2002; Liritzis et al., 2004) is termed SIMS-SS since the primary input variable, which controls the water in the mass of obsidian, is the saturation achieved in the surface layer (SS). This method is similar to ODD-SIMS (Anovitz et al., 1999; Riciputi et al., 2002) but differs in the manner in which profile is modeled. There are two advantages to our new procedure: (1) the final shape of the hydrogen profile incorporates two of the principal external and highly variable environmental parameters, those of temperature and humidity; (2) the use of SIMS instrumentation to measure surface hydration layers results in high precision thickness values with an error of 1-5 % depending upon the degree of surface roughness.

It has been demonstrated the accuracy of this method comparing obsidian SIMS-SS ages from well-known archaeological contexts with radiocarbon ages. Both forms of material within the deposit (e.g., carbon, obsidian) reflected, as closely as possible, the same depositional event and depositional history (Liritzis et al., 2004; Liritzis & Diakostamatiou, 2002; Liritzis & Diakostamatiou, 2006).

In this paper, we review and reassess the procedure for obsidian age estimation that is based upon the depth and shape of the hydrogen diffusion profile as determined by secondary ion mass spectrometry (SIMS) and clarify some points of accuracy in the age calculation, proposed earlier (Liritzis & Diakostamatiou, 2002; Liritzis et al., 2004).

The reassessment involves, 1) the determination of the saturated surface layer SS is determined more accurately through the first derivative of dC/dx of the initial part of the sigmoid profile of concentration C versus depth, x, combined with the successive linear regressions, 2) the whole computational procedure for age calculation has been formulated in a friendly used software based on MATLAB, which includes also the overall error (error propagation), and 3) the best but effective too fitting to the H^+ profile is the 3rd order polynomial with the best R-squared test.

WATER DIFFUSION IN OBSIDIAN

The diffusion of water in obsidian takes place with two mechanisms (Fig.1).

The first mechanism, is through the external surface of obsidian which is in direct contact with its surroundings. This mechanism is defined as the initial mass transport between a layer of resistance on the surface, from the surroundings to the external surface

The second mechanism, is the transport of the water into the obsidian mass, in other words, the diffusion of water in obsidian.

It should be stated that the first mechanism is the mass transport through a film on the surface. The mass transport in this surface

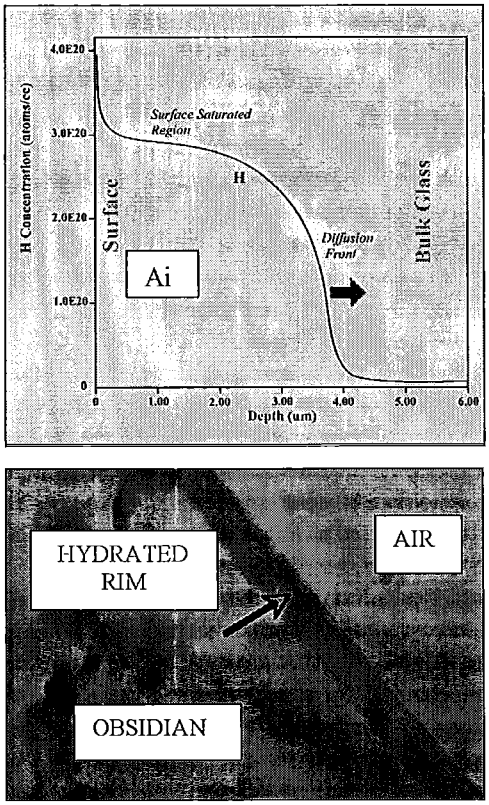

Fig.1: a) Schematic representation of water diffusion in obsidians, b) hydration rim of thickness in obsidian blade of 10 μm.

film is much faster than the mass transport in the solid body. This phenomenon is due to the fact that, in the first case, the humidity transport from the surrounding is made through the air layer, existing between the surrounding and obsidian. This air layer exerts much smaller resistance to water diffusion than the solid obsidian.

The mass transport essentially takes place once the molecules of the diffusing material are transported into the mass structure of the material. The ability for this transport, that is the existing resistance to the diffusion, depends upon the intermolecular distance of this material compared to the size of the molecules of the diffusing material. Since the diffusing compound is the same, the rate for the transport of the diffusing material differs considerably for the transport within the solid, compared with that within the liquid or gas medium. Therefore the transport rates are much faster within the air medium than the liquid and much more than in the solid (Brodkey et.al. 1988).

The size-dependent mechanism has been reviewed elsewhere (Liritzis & Diakostamatiou, 2006).

The diffusion rate of water in amorphous silicates is strongly correlated with the concentration of water within the surface hydration layer (Drury et al., 1962; Lee et al., 1974; Nogami & Tomozawa 1984) and is referred to as concentration-dependent diffusion. When dealing with a narrow compositional range, the anhydrous component of the glass has little influence on the mobility of water (Behrens & Nowak 1997). Under ambient temperatures (0-30°C) the diffusion of water in obsidian is not a steady state diffusion process with a constant D, and cannot be mathematically estimated with Fick's first law. Instead, as water enters the glass network the structure is depolymerized and allows additional water to enter the glass at a faster rate. This changing diffusion coefficient results in the formation of a characteristic S-shaped concentration-depth profile (Anovitz et al., 1999; Lee et al., 1974; Tsong et al., 1978).

As a result of the above, traditional age equation (x^2 = K.t, K= diffusion rate, t = time and x = hydration depth) is longer valid and alternate modeling procedures were required.

However, for a given obsidian and local environment (i.e. depending on the Archaeological site), the saturated concentration of water in the surface remains constant after a few years, and the thickness of the saturated layer increases with time according to a Fickian law of diffusion. The recognition of a non-Fickian diffusion in obsidian has led to finite

difference numerical solutions (Anovitz et al., 1999; Riciputi et al., 2002). However, this has been analytically described with transport phenomena (Brodkey and Liritzis, 2004), and our dating approach follows the *phenomenological method,* which starts with the assumption of Fickian diffusion law, as a possible improvement over empirical methods. In an earlier paper it was pointed out that there are really two regions in the SIMS diffusion profiles –the initial part and that following the convex point- where only the 2nd part seems to comply with Fick's law (Brodkey & Liritzis, 2004). Further assumptions in our model include the exponential dependence of diffusion coefficient D with C, but the adopted basic concept is the surface saturation layer in diffused media to solids. Further refinement of this method would be the use of purely scientific approaches to explain the diffusion.

DIFFUSION AND SURFACE SATURATION (SS) LAYER

The study of the water diffusion in obsidian is based on the assumption that the diffusion goes forward only in one direction, the direction x, which is perpendicular to the external surface of the obsidian sample (Liritzis & Diakostamatiou, 2002). It is considered that the diffusion system of water-obsidian is a semi-infinite diffusion system. This is justified by the fact that on one side of the system (external surface) there is the specified surface concentration of the saturated layer (Friedman & Long 1976), while on the other side is the solid mass of obsidian that represents the infinite direction. The diffusion process is shown in Fig.1.

Consequently, as the diffusion of the water from the surrounding to the external surface of obsidian is much faster than the diffusion of water within its mass, an external surface layer of obsidian becomes saturated in water within a short period of time (Brodkey & Liritzis, 2004). As the water diffuses further

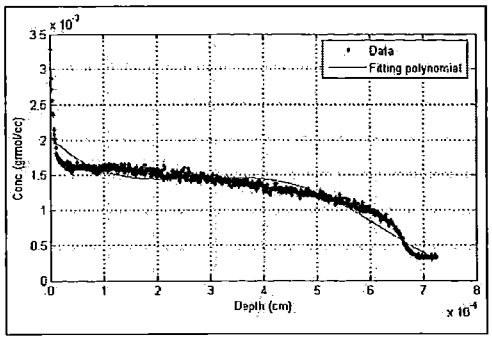

Fig.2: SIMS profile and best fitting 3rd order polynomial.

in obsidian, the profile of the water concentration C, versus the diffusion distance, x, has a sigmoid (S-like) shape (Fig.2) (Tsong et al. 1978, Lee et al. 1974, Anovitz et al. 1999, Stevenson et al. 2001, 2002).

The combined factors of the faster diffusion rate of water in the obsidian surface, together with the kinetics of the diffusion mechanism for the water molecules, and the specific amorphous texture of obsidian, as well as the external conditions for the diffusion (temperature, relative humidity, pressure, (Smith et.al. 1987), all result in the formation of an approximately constant, boundary concentration value, in the external surface layers. This is the surface saturated layer (SS layer), in the plot of C versus x. (Liritzis & Ganetsos, 2005 a).

The following important observation can be drawn from the H^+ profiles: although broadly they are quite similar, this is their only shared property, because despite the fact that they are derived from the same source and are of adjacent age, close inspection of the shape of the corresponding profiles suggests definite differences (see Figs.3 a-6 a).

The above remark derives from the considerable impact environmental and intrinsic effects may have on the obtained form of the SIMS hydrogen (H^+) profile.

It is due to these effects that apparent variations in the obtained profile are case specific.

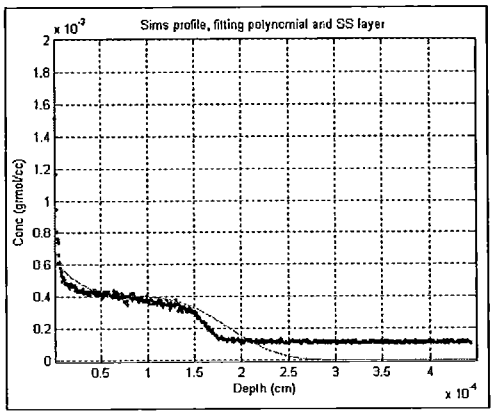

Fig.3 a. Easter Islands, Chile. SIMS profile, best polynomial fitting (solid line) and SS layer (bold data).

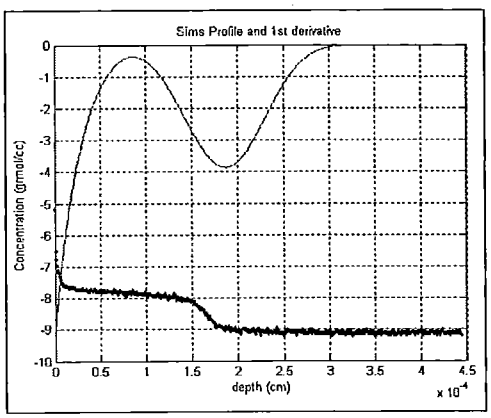

Fig.3 b. Easter Islands. SIMS profile and the 1st derivative of the fitted polynomial of Fig.3a.

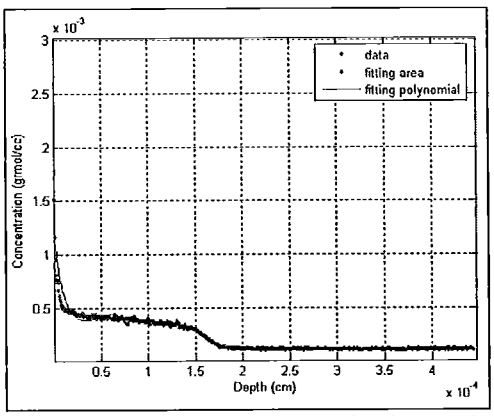

Fig.3 c. Easter Islands. SIMS profile, fitted area and fitted polynomial (solid line).

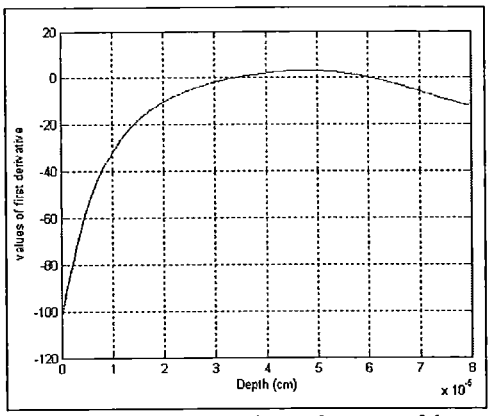

Fig.3 d Easter Islands. The 1st derivative of the polynomial fit of the initial part of the profile.

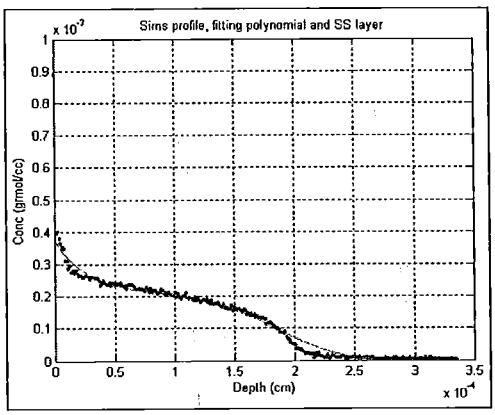

Fig.4 a. Mexico. SIMS profile, best polynomial fitting (solid line) and SS layer (bold data).

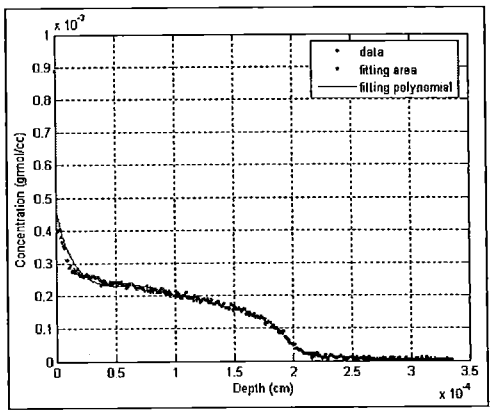

Fig.4 b. Mexico. SIMS profile and the 1st derivative of the fitted polynomial of Fig.4a.

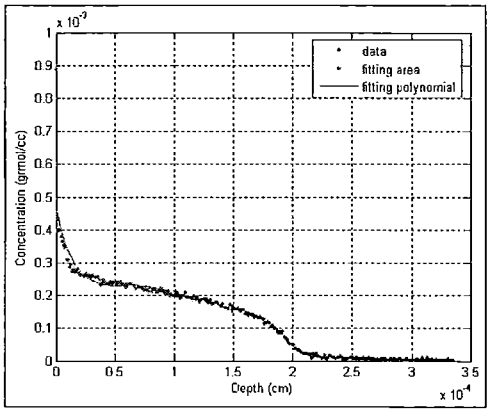

Fig.4 c. Mexico. SIMS profile, fitted area and fitted polynomial (solid line).

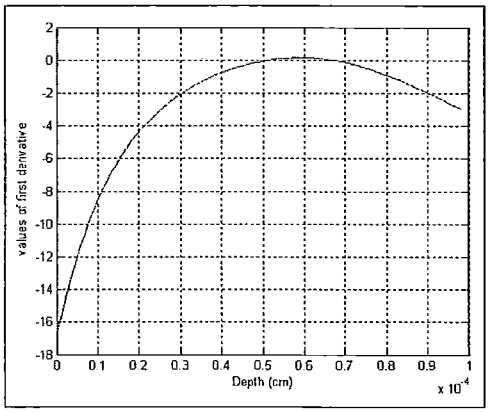

Fig.4 d Mexico. The 1st derivative of the polynomial fit of the initial part of the profile.

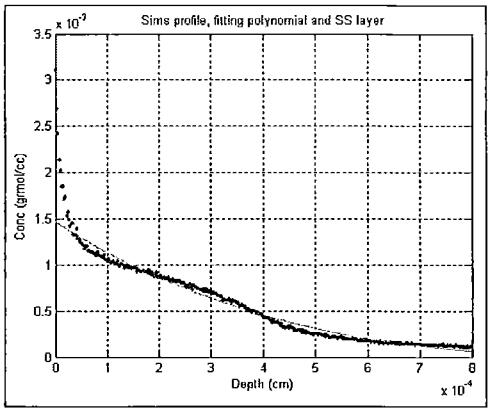

Fig.5 a. Mykonos. SIMS profile, best polynomial fitting (solid line) and SS layer (bold data).

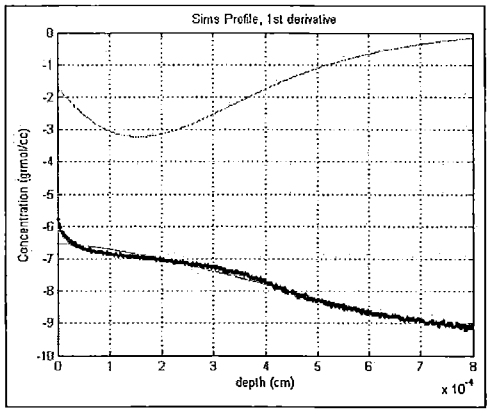

Fig.5 b. Mykonos. SIMS profile and the 1st derivative of the fitted polynomial of Fig.5a.

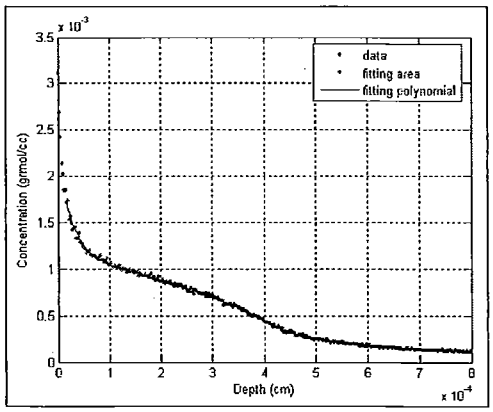

Fig.5 c. Mykonos. SIMS profile, fitted area and fitted polynomial (solid line).

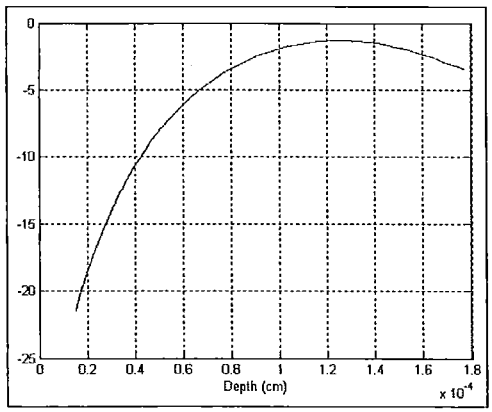

Fig.5 d Mykonos. The 1st derivative of the polynomial fit of the initial part of the profile.

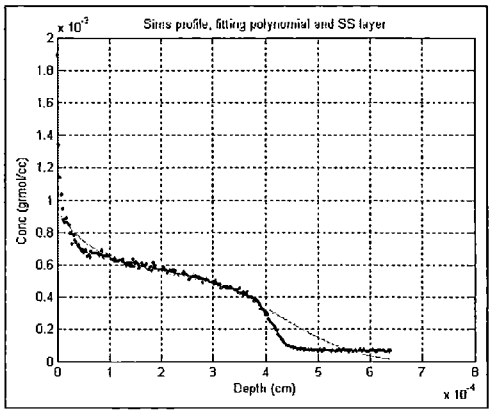

Fig.6 a Phylakopi at Melos. SIMS profile, best polynomial fitting (solid line) and SS layer (bold data).

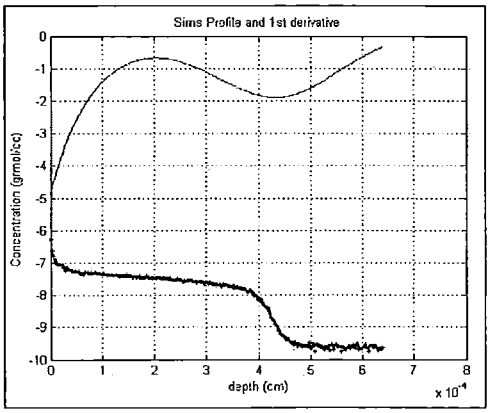

Fig.6 b. Phylakopi at Melos. SIMS profile and the 1st derivative of the fitted polynomial of Fig.6a.

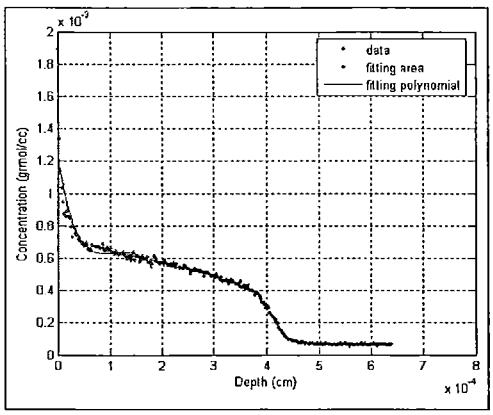

Fig.6 c. Phylakopi at Melos. SIMS profile, fitted area and fitted polynomial (solid line).

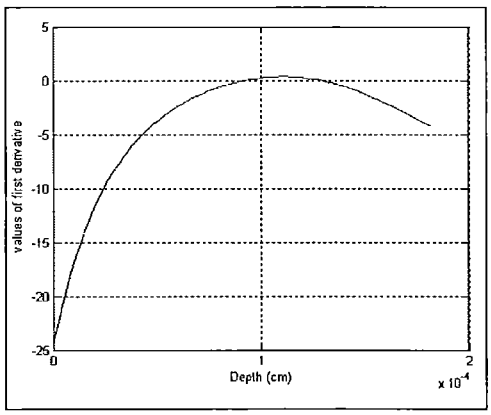

Fig.6 d Phylakopi at Melos. The 1st derivative of the polynomial fit of the initial part of the profile.

This is an important observation that the calculated age by SIMS-SS method relies on. Therefore, any age calculation is based on this diffusion profile, which is unique for every obsidian sample.

DERIVATION OF THE AGE EQUATION

The diffusion of environmental water into obsidians depends on random molecular motion but with the tendency for water to move in the direction of decreasing water concentration (x-axis vertical to obsidian's surface). The rate of this movement also depends on temperature, relative humidity and the location and arrangement of ions within the obsidian structure. The result is a sigmoid shape water (hydrogen ions) concentration profile that incorporates all variations of the external parameters into the final profile shape (Fig. 2). Using this end product of diffusion, we have developed a phenomenological model, based on certain initial and boundary conditions and physicochemical mechanisms, that expresses the H_2O concentration versus depth profile as a diffusion/time

equation. This allows chronometric ages to be calculated. The mathematical review of the diffusion age below is based on Liritzis et al., (2004).

We model this diffusion process as one-dimensional phenomena, where water molecules enter a semi-infinite medium in a direction perpendicular to the surface. The model is based on the idea that in the saturated surface (SS) layer encountered near the exterior of the sample (i.e., in the first half of the sigmoid curve), the concentration (C) of molecular water is assumed as constant along a very short distance. Thereafter, C decreases gradually following the trend of the sigmoid curve

The mathematical theory of diffusion in isotropic substances is based on the observation that the rate of transfer of the diffusing substance, through a unit area, is proportional to the concentration gradient measured normal to the section. It is expressed by the equation:

$$F_x = -D\,\partial C/\partial x \qquad (2)$$

where: F_x is the rate of transfer of water moles per unit area (kmol m^{-2} s^{-1}) along x-direction, C the concentration gradient of diffusing substance (mass per unit volume) acting as the driving force, x the distance coordinate measured normal to the section, and the proportionality constant D is called the diffusion coefficient (m^2 s^{-1}) or less commonly as molecular mass diffusivity or just mass diffusivity. The negative sign arises because diffusion occurs in the direction opposite to that of increasing concentration. It is combined with the flux as D = flux / gradient, where gradient is the dC/dx of the concentration versus depth profile.

For the use of diffusion for dating it is essential to establish the time that diffusion has occurred. For this, complex dynamic or time-dependent analysis is required rather than simple steady state. Hence, the concept of property balance is introduced, whereas, input ($\partial C/\partial t$) + generation = output (C) + accumulation ($\partial(D\partial C/\partial x)$). In considering this case of one-dimensional diffusion through an obsidian surface, where there is a concentration gradient along the x-axis, the diffusion coefficient (D), as a function of change in C with time, will be variable, and it is derived from the partial differential equation:

$$\partial C/\partial t = \partial\,(D\partial C/\partial x)/\,\partial x \qquad (3)$$

which is a combination of eq. (2) for non-steady state condition with the balance equation concept for no flow or generation, where: t=time and x = distance. It denotes the rate of change of C with time (t), which equals a diffusion coefficient by the rate of change of C along X-axis. In fact D relates C(t) with C(x), and has the significance that it is the contribution to the rate of transfer in the x-direction due to the component of C gradient in this direction.

For constant D equation (1) becomes:

$$\partial C/\partial t = D(\partial^2 C/\partial x^2) \qquad (4)$$

that is, there is a gradient of C only along the x-axis, and the rate of change of C with time (t) equals the rate of transferred water molecules per unit distance (x) times the rate of change of C divided by x. Equations (2) and (4) are usually referred to as Fick's 1st and 2nd laws of diffusion by direct analogy with the equations of heat conduction.

It has been shown (Crank, 1975) that Equation (4) produces several numerical solutions depending on the system's initial and boundary conditions. For the present obsidian-water system, an exponential diffusion coefficient is modeled under the constraints, where:

Initial conditions: $C=C_o=Ci$, where Ci is the initial or structural water concentration of the glass; x equals the diffusion depth, where $x>0$; for a diffusion time, $t=0$.

Boundary condition: $C=C_s$ the obsidian surface (saturated) water concentration, for $x=0$ and $t>0$.

However, in concentration-dependent diffusion, D is not constant during the hydration process but depends on changes in C. A family of curves that relates concentration-to-distance for an exponential diffusion coefficient during sorption is given (see, Fig.2 in Liritzis et al., 2004), which, through linear interpolation, are based on those given by Crank (1975). Additional curves have been added (see, Fig.3, in Liritzis et al., 2004) and developed to accurately estimate k-value (of e^k). They represent calculated results for variable diffusion coefficients for non-steady-state conditions. It follows that the form of exponential dependence of the C from D is given by exponential equation:

$$D=D_s \exp(kC/C_s)= D_s\exp[\beta(C-C_s)] \quad (5)$$

where: k= a constant, D_s the diffusion coefficient (=1/gradient) for $C=C_s$ and β= a constant.

In fact, Boltzmann (Boltzmann, 1894) showed that for certain boundary conditions, provided D is a function of C only, C may be expressed in terms of a single variable and that Equation (3) may be reduced to an ordinary differential equation by the introduction of a new variable.

Based upon Crank's (1975) numerical solutions of diffusion, and Boltzmann's transformation, the following auxiliary variables are introduced:

$$y_s=x/2(D_st)^{1/2}, \quad (6)$$

$$c=(C-Cs)/(C_i-C_s) \quad (7),$$

where Ci the initial concentration (pristine water) in obsidian prior to diffusion of water, and,

$$\gamma=\beta(Ci-C_s) \quad (8)$$

Then eq.(5) becomes,

$$D=D_ie^{\gamma} \ (D_i \text{ at } C=C_i) \quad (9).$$

Substitution of equations (6), (8) and (9) into (3) we obtain

$$d(e^{\gamma}d\gamma/dy_s)/dy_s + (2y_s)(d\gamma/dy_s) = 0 \quad (10)$$

In view of the boundary condition, eq.(6), and eq.(8), the integration of eq.(10) is to be performed with $\gamma=0$ and $y_s=0$. Thus, we can use the values of γ calculated from eq.(10) .

In view of initial condition for C=Ci, the eq.(7) and eq.(8), we have,

$$\gamma=\beta(Ci-C_s)=r, \ y_s=\infty \quad (11)$$

$$c = \gamma/r \quad (12)$$

Here, it is,

$$r = \log(D_{C=Ci} / D_{C=Cs}) \quad (13)$$

(Indeed, $D_{(C=Ci)}=D_{(C=Cs)}\exp(\beta(C_i-C_s)) \rightarrow D_{(C=Ci)} / D_{(C=Cs)} = \exp(\beta(Ci-Cs))$, and $\log[D_{(C=Ci)} / D_{(C=Cs)}] = \beta(Ci- Cs) = r$)

From eq.(13) and eq.(5) we define

$$r= kC/Cs \quad (14)$$

Therefore, we use the exponential form $D_{(C=Ci)}=D_{(C=Cs)}\exp(kCi/Cs)$ upon which the concentration-distance curves, are based (see below, Curve fitting- Choosing the best polynomial).

Plotting the values of r (i.e. the limiting values of γ at $y=\infty$), as a function of auxiliary parameter g used for the integration of eq.(10) (for $u=e^{\gamma}$), numerical values of c are compiled. Solutions of eq.(10) from $y=-\infty$ to $y = +\infty$, for the initial conditions, $\gamma=0$, $u=1$, $y=0$, were obtained for different values of g given by $g=(d\gamma/dy)$ (for details, see Crank, 1975).

However, instead of using such plot one may calculate the g values with the aid of the following empirical interpolation formula:

$$g=(1.128r) / (1-0.177r) \quad (15)$$

Following Boltzmann's transformation, and using eq.(6) and eq. (7), the flux across the surface x=0 of eq.(2) becomes:

$$-D_s(\partial C/\partial x)_{x=0} = -1/2(D_s/t)^{1/2}(C_i-C_s)(dc/dy_s)_{ys=0} \quad (16)$$

From $g=(d\gamma/dy)$, eq.(12) and eq.(15), it follows that the dc/dy_S for $y_s=0$ is given by:

$$dc/dy_s=g/r=1.128 / (1-0.177r) \quad (17)$$

where, r is calculated from eq.(13).

Equation 16 relates the flux across obsidian's surface at x=0 with the time the flux has occurred, the C_s, the C_i and D_s for C_s.

It is only when, a) the initial and boundary conditions are expressible in terms of y_s alone, b) the x and t are not involved separately, c) diffusion occurs in semi-infinite media, and d) initial water concentrations are uniform (and may be zero) as it occurs in obsidian, that the transformation of eq.(6) and eq.(10) can be used.

It is necessary to clarify that the variation of C during sorption depends on various factors (environmental, such as, temperature and humidity, atomic structure and chemistry in obsidian, and the chemistry between burial environment and obsidian surface).

This variation reflects a respective variation in D. But, the variation of C with distance (hence time) presumably incorporates all these factors.

The idea put forward (Liritzis & Diakostamatiou, 2002; see, also Liritzis & Diakostamatiou, 2006) is that the obtained sigmoid shape of C versus (X) incorporates all these unknown factors as an end product of all processes, which lead the diffusion. It is also assumed that since we are dealing with a compact solid material, the diffusion profile has not changed significantly with time, the material being buried in the natural environment. In this case the environmental variations are not so radical and so long, in order to cause a significant alteration to the diffusion profile.

CURVE FITTING-CHOOSING THE BEST POLYNOMIAL AND LOCATION OF SS LAYER

In order to model the form of the diffusion profile a value for the constant K (or k) of eq. (14) must first be determined.

In Liritzis and Diakostamatiou (2002) this was fixed by the shape of the experimental curve that closely corresponds to Crank's (1975) theoretical curves. For the non-steady state condition considered here, a collection of sigmoid shaped curves have been produced for non-dimensional distance and concentration that reflect different values of K. In fact, the non-dimensional plot of X/X_o versus C/C_o given by Crank (1975) (his Fig. 9.9), includes some curves, where the parameter that defines each curve is the term e^k. For a full coverage of K-values, we have produced intermediate curves by linear interpolation (Liritzis et al., 2004). Exact estimation of K-values is produced from family curves of e^k versus X/X_s for certain C/Cs, by interpolation.

SIMS profiles were re-plotted as non-dimensional (standardized to 1) diagrams of C/C_s versus X/X_s and were matched to the appropriate profile of our produced curves guided by the end point of C along the x-axis. This way the k-value can be calculated from any particular sigmoid shape.

Subsequently, a curve is fitted to the SIMS data (Fig.2) using TABLECURVE 2D software and takes the form of a polynomial with exponential terms:

$$C=\exp (a+bx^{n-2}+cx^{n-1}+dx^n) \quad (18)$$
for n=3

The choice of the fitted curve is important for the age determination of the SS layer, due to the following three criteria: 1) our goal is to achieve the best fitting curve especially for the first portion, or upper half, of the S-like curve. This is a required in order to closely model the shape of the theoretical exponential diffusion

curves of the C versus x non-dimensional plots; 2) the upper half represents the (calculated) gradient of the fitted curve, which corresponds to the surface diffusion coefficient D_s, (i.e., the coefficient for the constant concentration of the saturated layer); and 3) the fitting should be congruent with the tail of the sigmoid curve.

Needless to say that this initial part of the sigmoid curve follows a different diffusion mechanism than the latter part to the end and that in comparing the experimental and theoretical curves, the initial points near the surface must be discarded (Brodkey, Liritzis & Diakostamatiou 2003).

To do this, the first points on the SIMS profile, for x>0, are removed gradually and up to the point that concentration ceases to drop, searching for the best fitted curve which satisfies the above criteria.

When the 3rd degree exponential polynomial curve is found, the SS was defined from the sliding successive linear regressions of the raw data sets (Liritzis & Diakostamatiou, 2002; Liritzis et al., 2004). The smallest gradients (ideally should be a zero gradient within error range of the data points) are met with linear regressions that define the plateau (SS layer) level. In fact, these appear along a band of less than 10% spread.

This tedious work is simplified by taking the 1st derivative of the 3rd order polynomial fitting of C versus X profile, the peak of which defines the uppermost region of the saturated layer. Then another best fit polynomial is taken for the initial part of the sigmoid profile up to the earlier found peak.

The choice of a 3rd order polynomial, rather than higher order exponential polynomial, was chosen to satisfy the three criteria for fitting of the initial and end points, as well as the first half of the S-curve. Overall, the higher order polynomial fitting seems better but at the expense of the criteria, particularly with the unavoidable presence of more oscillations. This was reinforced in practice during the applied trials and blind tests whereas the 3rd order polynomial gave the best results.

Subsequently, the sliding linear regressions of the data points between the two peaks of the 1st derivatives locate the SS layer: it is the maximum data length with smallest slopes. Smallest slope corresponds to a hydration depth after which slopes drop to monotonously negative values implying diffusion to deeper obsidian hydrated layers.

Having defined the fitted curve, the inverse of gradient dC/dx (or tangent at a certain point of the fitted curve), or from another point of view, the inverse of rate of change, is assumed to be related to the diffusion coefficient, D:

$$D = 1/dC/dx = 1 / [(b+2cx+3dx^2) \exp (a+bx+cx^2+dx^3)] \quad (19)$$

Where, effective D was found and expressed from the calculated data of eq.(23) below.

AGE EQUATION

Taking into account the abovementioned diffusion phenomenon of water in obsidian and solving equation (16) the following dating equation is obtained. This is the diffusion time (=age):

$$T = [(C_o - C_s)^2 (1.128/(1-0.177kC_o/C_s))^2] / [4D_{s,eff}(b*\exp(a))^2] \quad (20)$$

where C_o is the initial concentration of the intrinsic water in obsidian,

C_s the constant surface concentration of water to the saturated layer,

k the constant factor that corresponds to the non-dimensional curve which characterizes the certain diffusion profile, according to Crank (1975), where k-values presented as e^k are derived from a family of curves of e^k versus X / X_s for certain C / C_s, where

$$D = D_s \exp(kC/Cs) \quad (9)$$

X_s is used in the calculations of the gradient dC/dx of the C vs. X profile. For $C = C_s$ and $X = X_s$ we set diffusion coefficient $D = D_s$. According to 1st Fick's law Ds is the inverse of gradient, thus it is:

$$(\partial C/\partial x)_{X=0} = b*\exp(a) \quad (21)$$

and

$$D_s = (\text{flux} / \text{gradient}) \times 10\text{E-}11 \text{ years} \quad (22)$$

In the calculation of D the multiplication 10E-11 has been performed in order to convert units of D from the calculated μm^2/1000 years to cm^2/year ($\mu m^2 = cm^2 10^{-8}$ and $\mu m^2/10^3$ years = $cm^2 10^{-8}/ 10^3$ years = $cm^2 10^{-11}$ / year), which are the units used in SIMS-SS

For $X=X_s$ (average of max defined length of SS layer), D_s is computed from eq. 22.

However with D_s the age is far from right. It is well known that the diffusion coefficient is a diffusion constant, which could be derived mostly from the experimental data (Brodkey et.al. 1988). Therefore, a relationship should be devised relating the coefficient D_s to an effective coefficient $D_{s,\,eff}$. That is, D_s / $D_{s,eff}$ versus D_s x 10E11.

The empirical $D_{s,\,eff}$ is determined for obsidians with well known archaeological age.(t). Then, the obtained relationship, using TableCurve 2D, is of the type $y^{-1} = a + b / x^2$; it is constructed from 26 different dated samples and becomes eq. (23).

$$D_{s,eff} = a*D_s + b/(10^{22}*D_s) \quad (23)$$

where, a= 8.051E-6, b= 0.999, ($r^2 = 0.999$).

Equation (20) gives the diffusion time, which includes the time required for the formation of the saturated layer, the depth X_s and the concentration C_s. Needless to say that the SS layer formed with a highest concentration and a progressing front during the diffusion time is defined from C_s and X_s.

THE NEW SOFTWARE OF SIMS-SS

The program was created as a *GUI* (Graphical User Interface) by using the *guide* (Graphical User Interface Development Environment) of Matlab. *GUI* is a pictorial interface to a program (Chapman, 2004). A good GUI can make programs easier to use by providing them with a consistent appearance, and with intuitive controls such as pushbuttons, edit boxes, list boxes, sliders, and menus. Our program is separated into three parts. The first part is the main window which appears when the program starts and also contains the code for the age calculation. Here there are eight pushbuttons sorted, in order the user to use them one by one without getting confused. They are in the middle of the window and separate the window into two panels. Left panel is there were the user has to enter the area for the linear regression and the coefficients of the fitting polynomial. Right panel is the output panel of results. The second part is the window that appears when the user push the button "calculate points" and is used for the approximate location of the SS through the criterion of first derivative. The third part is the window which appears when the button "Fitting poly" is pressed and is used for the calculation of the best fitting polynomial.

The program is written in Matlab version 7.0.1 and runs under windows 2000 or newer with the help of the *MCR* (Matlab Component Runtime). In order to become distributable it is needful to use the Matlab command *mcc*. This command Prepare a program for deployment outside of the Matlab environment. Generate wrapper files in C or C++ and optionally build standalone application with extent "*.exe*". Before end users can run Matlab Compiler-generated components on their machines, they need to install the MCR, if it is not already present. MCR is a standalone set of shared libraries that enables the execution of *M-files*.

When *guide* is executed, it creates the Layout Editor. The layout editor window has a palette of GUI components along the left-hand side of the layout area. A user can create any number of GUI components by first clicking on the desired component and then dragging its outline in the layout area.

The steps taken to write the novel software are as follows:

1. We decide what elements were required for the program and make a rough layout of the components by hand on a piece of paper.
2. We used the Matlab tool called *guide* and lay out the components on a figure.
3. We saved the figure to a file. When the figure was saved, two files was created on disk with the same name but different extents. The *fig* contains the GUI layout and the components of the GUI; the *M-file* contains the code to load the figure along with skeleton callback function for GUI element.
4. We wrote the code to implement the behavior associated with each callback function
5. We used the command *mcc* to create a stand-alone application capable for distribution.

The following steps refer to the data elaboration in some detail.

1) At menu, first we choose "File", and then we choose "Load" and by using the standard loading interface of windows, we open a "txt" type of file, containing our data in two columns; one for depth in ?m and one for concentration in atoms/cc. Subsequently, the programs draws a graph of SIMS profile for Concentration (in grmole/cc), versus, depth, x (in cm).

2) From fitting tests so far we know that the best polynomial to describe the SIMS profile is the 3rd order polynomial (Liritzis et al., 2004). A statistical way to find the best fitted polynomial is by using R-squared test. R-squared measures how successful the fit is in explaining the variation of the data, as a measure of the square of the correlation between the response values and the predicted response values. Appropriate algorithm can change the four polynomial coefficients until the r-squared becomes maximum. The polynomial which gives the maximum R-sq is used in step (3) in order to calculate the 1st derivative.

3) Calculate the length of the SS layer by linear regressions in a region defined by the criterion of the first derivative of the whole profile as well as the peak of 1st derivative of the initial part of the profile (from first points to the peak of 1st derivative). The time for doing linear regressions in all over the profile is approximately 15-20 minutes, but by using the 1st derivative criterion the procedure becomes faster and accurate. With the sliding linear regressions the concentration and the depth is computed.

As concentration is a variable of distance (depth), then the 1st derivative is the change of concentration with time. The SS layer is saturated, which means that concentration will be almost constant which is reached within a short period of time. Such SS layer is identified to a straight line between these peaks. Depending on the particular sigmoid shape the SS can be found either between the two peaks or around the peaks. Figs.3-6 show the SS layer by this way. The Xs is taken as the average of the max length of SS associated by their standard deviation. Then the program calculates and provides the values of C_s, X_s, C_i, at the output panel.

4) The last input in the age equation is the variable "k". To define this variable we compare a non-dimensional plot of SIMS profile with a family of curves. Non- dimensional plot is a plot where x-axis is depth value over the depth at SS layer (X/X_s), and in y-axis the concentration over concentration at

SS layer (C/C_s). It is very important to choose a theoretical curve that its tail ends in the same points as the tail of our non-dimensional data plot, where, k-values presented as e^k are derived from a family curves (see, fig.2 of Liritzis et al., 2004).

5) The final step is calculation of the age.

One important aspect about the construction of this software is that after every calculation the program transfers automatically the results on the right field. This is simply executed by clicking on the "calculate age" button.

6) "Save" is also another option in menu "file", for saving our results as a "txt" type of file, together with the array of the linear regressions.

SOME APPLICATIONS

Table 1 shows the age data calculated with the new software, for four archaeological obsidian samples. Dates are compared to archaeological ones and to earlier SIMS-SS calculations. They are concordant with archaeological / C-14 ages and earlier SIMS-SS calculations. Figures 3-6 give the plots related to the age evaluation per each sample case.

AGE ACCURACY DUE TO Xs, Cs, k AND Cint

The effect on age of the errors in individual parameters in age equation, such as those of Cs, Xs, Cint, k are shown in Figs (7-10). Fig.7 is the sensitivity of age with saturated concentration (Csur). We observe a linear effect of concentration C_S on age, where a $\pm$4% error on C_s gives an error of 7-8% on age.

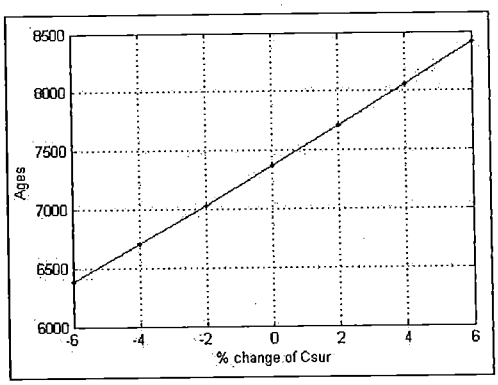

Fig.7 Effect of Cs on Age.

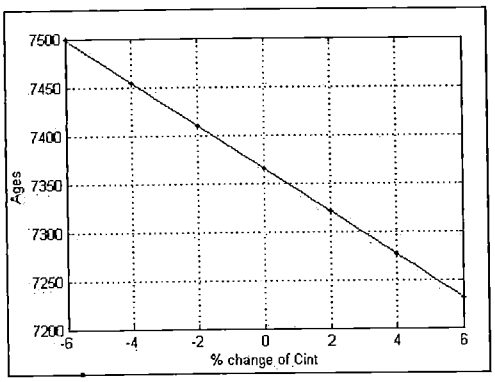

Fig.8 Effect of Cint on Age

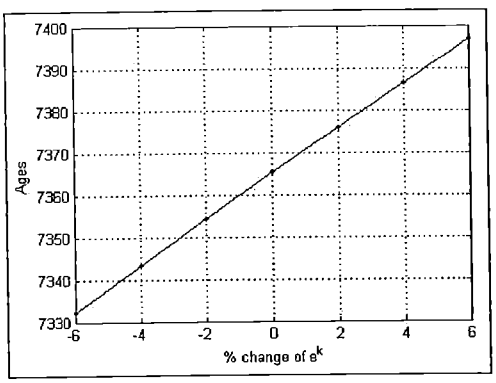

Fig.9 Effect of k-value on Age

Fig.8 is the sensitivity of age with initial concentration (C_i). The change of initial concentration also is linearly related with the age., and a $\pm$4% error in C_i gives an around $\pm$1.5% error in age. Fig.9 shows the sensitivity of age in relation to e^k, where age changes slightly for large K-value variation; a $\pm$4% in K-value gives the insignificant 0.3% error in age. Fig.10 is the exponential effect of X_s on age, which is the crucial parameter. An error

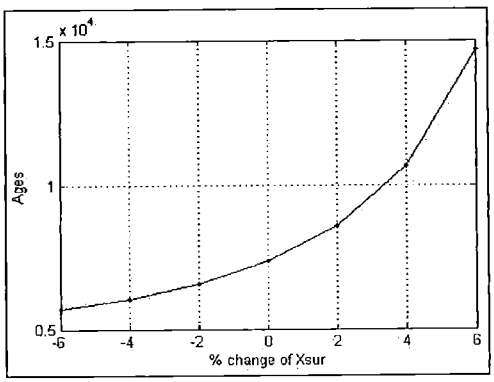

Fig.10 Effect of Xs on Age

of ±2% error in X_s provides around ±10-12% error in age.

The final age error is due to the error propagation of the age equation (20). Through experiments, we observe that the final error is approximately 2-4% of the final age. Most sensitive parameter is X_S, which depends on a) degree of surface flatness and smoothness (where the beam focus), b) depth profiler accuracy, and c) obsidian structure. Errors in all these vary between 1-7% .

SECONDARY ION MASS SPECTROMETRY

SIMS analyses were conducted at the commercial laboratory of Evans East, East Windsor, NJ, the profiles were collected using PHI Model 6300 and 6600 quadrupole-based secondary ion mass spectrometers. A 5.0 KeV Cs^+ primary ion beam with an impact angle of 60° with respect to surface normal was used and negative secondary ions were detected. Charge build up during profiling was compensated for by use of an electron beam. The ion signal was maximized by using the electron beam resulting in the least amount of charging. The measurements were performed using a 300 x 300 micron ion beam raster, which results in very little visual disruption to the sample surface. Generally, the SIMS depth scale accuracy is within 5-10%. This translates into an estimated error of ±0.05 μm. This value is not equivalent to the ±0.01-0.03 μm standard deviation usually associated with SIMS because of the irregular surface topography present on naturally cleaved samples. However for flat and smooth areas reproducible errors in depth are 2-3%.

The sputtering rate used to measure of our samples was 24 Angstroms/second, which is fairly typical. Conversion of ion counts to concentrations is done using an ion implanted obsidian standard. This standard has been used to calibrate the sputtering rate, therefore there are no direct crater depth measurements of archeological samples. This method adopted by Steve Novak provides very good control of the depth scale and avoids the problems of direct measurement of a rough surface. For polished test samples, crater depths are measured using a Dektak 6M stylus profilometer. It has been demonstrated that this instrument is reproducible to within 1% on flat, well-controlled samples (Novak and Stevenson, 2005, SIMS XV, Manchester 2005, Abstract Book, p.63).

CONCLUSION

The novel obsidian hydration dating method SIMS-SS has been reassessed with regards to alternative ways in the location of the surface saturation layer. Although the successive linear regressions carried out on the initial part of the sigmoid profile is retained, the length of data for this procedure is confined between two peaks defined by first derivatives of fitted polynomials. Moreover, the whole procedure of age calculation is simplified, has become faster, the intermediate calculated data are stored for later use and overall error, derived from error propagation, is attached in the computed age. Four earlier estimated ages are compared with present evaluation and the results are similar within error bars.

Table 1: Age data calculated with the new software, for four samples from the Aegean Sea, Mexico and Easter Islands. SS in Xs column is thickness of SS layer. Dates in numericals from earlier estimation: 1, Liritzis & Diakostamatiou, 2002; 2, Liritzis et al., 2004.

Site	Xs (cm)	Cs (grmole H_2O/cc)	Cint (grmole H_2O/cc)	k	Ds (cm^2/yr)	C14/ Archaeological date, years BP	SIMS-SS Years BP
Phylakopi Bronze Age site, Melos, Aegean Sea Code: 2000-145	1.11e-4 ± 7e-6 SS: 1.4e-5	6.4e-4 ±1.4e-5	6.57e-5 ± 3.3e-6	3.9	1.24e-12	4000-4500	4191±77 (4100+/-?)[1]
Ftelia neolithic site, Mykonos, Aegean Code: 2000-148	1.48e-4 ±1.9e-5 SS: 3.8e-5	9.74e-4 ±3.9e-5	0.000113 ±5.6e-5	3.4	2.69e-12	6500-7100	7106±148 (6720+/-?)[1]
Xaltocan Mexico Code: 1993-199	8.19e-4 ±1.1e-5 SS: 2.2e-5	2.21e-4 ±8.1e-6	2.12e-6 ±2.8e-6	2.3	4.35e-13	955-1250	1035±26 (1020+/-?)[2]
Easter Islands, Chile Code: 1993-82	5.17e-5 ±8.2e-7 SS: 1.6e-5	4.16e-4 ±3.1e-6	1.08e-4 ±4.4e-6	3.9	1.29e-12	310-522	415±12 (543+/-30)[2]

ACKNOWLEDGEMENTS

We thank ERMIS General Secretariat for Research & Development, Ministry of Development for financing this ongoing Project and for partial cost of this volume.

REFERENCES

Anovitz, L.M., Elam, J.M., Riciputi, L.R. and Cole, D.R. (1999) The failure of obsidian hydration dating: sources, implications, and new directions, *Journal of Archaeological Science*, vol. 26, 735-52.

Behrens, H. & Nowak, M. (1997) The mechanisms of water diffusion in polymerized silicate melts, *Contributions to Mineralogy and Petrology*, vol. 126, 377.

Boltzmann, L.(1894) *Annln Phys.*, vol. 53, 959.

Brodkey, S.R. and Hershey C.H. (1988) *Transport Phenomena A Unified Approach*, edited by Clark B.J., McGraw-Hill., Singapore.

Brodkey, R.S., Liritzis, I. and Diakostamatiou, M. (2003) Transport phenomena and archaeology: application to obsidian hydration dating. *Intern. Workshop, Melos island, Greece, 2-6 July, 2003,* University of the Aegean and IAOS, Rhodes, (Abstract Book, p.13).

Brodkey, R. S. and Liritzis, I. (2004) The dating of obsidian: a possible application for transport phenomena: a tutorial. *Mediterranean Archaeology & Archaeometry*, vol. 4 (2), 67-82.

Chapman, S. (2004) *Matlab programming for Engineers*, 3rd Edition, Nelson, Ontario.

Crank, J. (1975) *The Mathematics of Diffusion*, 2nd Edition, Oxford University Press., New York.

Drury, T., Roberts, G. J. (1963) Diffusion in silicate glass following reaction with tritiated water vapour, *Physics & Chemistry of Glass*, vol. 4, 79-90.

Lee, R. R., Leich, D. A., Tombrello, T. A., Ericson, J. E. and Friedman, I. (1974) Obsidian hydration profile measurements using a nuclear reaction technique. *Nature*, vol. 250, 44-47.

Liritzis, I., Diakostamatiou, M. (2002) Towards a new method of obsidian hydration dating with Secondary Ion Mass Spectrometry via a surface saturation layer approach, *Mediterranean Archaeology and Archaeometry*, vol. 2(1), 3-20.

Liritzis, I., Diakostamatiou, M, Stevenson, C.M, Novak, S and Abdelrehim, I. (2004) Dating of hydrated obsidian surfaces by SIMS-SS. *J. Radioanal. Nucl. Chem.*, vol. 261 (1), 51-60.

Liritzis, I. and Ganetsos, T. (2005a) Obsidian hydration dating from SIMS H+ profiling based on saturated surface (SS) layer using a new software. In *SIMS XV*, Manchester 2005, Abstract Book, p.62 (Refereed Proceedings, in press)

Liritzis, I and Diakostamatiou, M. (2006) SIMS-SS, a new obsidian hydration dating method; analysis and theoretical principles. *Archaeometry* (in press).

Mazer, J., Stevenson, C., Ebert, W. & Bates, J. (1991) The exponential hydration of obsidian as a function of relative humidity and temperature. *American Antiquity*, vol. 56, 504.

Nogami, M. & Tomozawa, M. (1984) Diffusion of water in high silica glass at low temperature. *Physics and Chemistry of Glass*, vol. 25, 82-85.

Riciputi, L., Elam, J. M., Anovitz, L. M., Cole, D. R. (2002) Obsidian diffusion dating by secondary ion mass spectrometry: a test using results from mount 65, Chalco, Mexico, *J. Archaeological Science*, vol. 29 (10), 1055-1075.

Smith, J. M., van Hess, H. C. (1987) *Introduction to Chemical Engineering Thermodynamics*, Fourth edition, McGraw-Hill, New York.

Stevenson, M. C., Liritzis, I., Diakostamatiou, M. (2001) A preliminary report of the hydration dating of Melos, Yiali and Antiparos obsidian. *Proceedings of the first International Conference "Hyalos-Vitrum-Glass"*, April 2001, Rhodes, Greece.

Stevenson, M. C., Liritzis, I., Diakostamatiou, M., Novak, S.W. (2002) Investigations towards the hydration dating of Aegean obsidian, *Mediterranean Archaeology and Archaeometry*, vol. 2(1), 93-109.

Tsong, I. S. T., Houser, C. A., Yusef, N. A., Messier, R. F., White, W. B., Michels, J.W. (1978) Obsidian Hydration Profiles Measured by Sputter-Induced Optical Emission, *Science*, vol. 201, 339-341.